Functional nanostructures and interfaces of strontium ruthenates $Sr_3Ru_2O_7/Sr_2RuO_4$ eutectic crystals

R. Ciancio,[1,2]* H. Pettersson,[2] J. Börjesson,[2] S. Lopatin,[3] R. Fittipaldi,[1] A. Vecchione,[1] S. Kittaka,[4] Y. Maeno,[4] S. Pace,[1] E. Olsson[2]

[1]Department of Physics "E.R. Caianiello," University of Salerno and CNR-INFM SuperMat Regional Laboratory, Baronissi (SA), Italy; [2]Department of Applied Physics, Microscopy and Microanalysis, Chalmers University of Technology, Göteborg, Sweden; [3]FEI Company, Achtseweg Noord 5, Eindhoven, The Netherlands; [4]Department of Physics, Graduate School of Science, Kyoto University, Japan

Vincitrice del Premio Carla Milanesi 2009

Corresponding author: Regina Ciancio
IOM CNR, Laboratorio TASC, Area Science Park, Basovizza S.S. 14 Km 163.5 34149 Trieste, Italy
Tel.: +39.040.3756467 - Fax: +39.040.226767
E-mail: ciancio@tasc.infm.it

Summary
Ruddlesden Popper Sr_n+1Ru_nO_{3n+1} ruthenates exhibit a wide variety of exceptional properties providing an ideal playground to study new forms of ordering effects such as superconductivity in Sr_2RuO_4. A new normal metal $Sr_3Ru_2O_7$/superconducting Sr_2RuO_4 eutectic system has been successfully grown. Transport and magnetic studies on the eutectic material revealed the presence of an unexpected superconducting behaviour in the $Sr_3Ru_2O_7$ domain. Several scenarios have been proposed to explain this unusual behaviour addressing the crucial need of a detailed investigation by local probe techniques. We report the nanostructural characterisation of the $Sr_3Ru_2O_7/Sr_2RuO_4$ eutectic crystals by transmission electron microscopy and high angle annular dark field scanning transmission electron microscopy. We compared the nanostructure of the $Sr_3Ru_2O_7$ region of the eutectic with that of $Sr_3Ru_2O_7$ single-phase crystals in which no superconducting behaviour has ever been observed. We found that $Sr_3Ru_2O_7$ can be grown with higher purity via eutectic solidification showing only a diluted amount of randomly dispersed Sr_2RuO_4 layers. We also explored the $Sr_3Ru_2O_7/Sr_2RuO_4$ interfacial nanostructure. Two typologies of interfaces are observed within the eutectic: interfaces parallel to the growth direction are sharp and defect-free whereas interfaces perpendicular to the growth direction appear wavy and decorated with Ru precipitates. An exotic pairing between the Sr_2RuO_4 layers finely dispersed in the $Sr_3Ru_2O_7$ matrix is suggested as possible scenario for the unusual superconductivity of the $Sr_3Ru_2O_7$ domain of the eutectic.

Key words: Ruthenates, eutectic structure, HRTEM, HAADF.

Introduction

One of the most exciting developments of modern condensed-matter physics has been the discovery of new forms of order in materials with strong electron-electron interactions. The past decade has seen the observation of a whole range of novel superconducting, magnetic and metallic states. In many cases these new states are subtle and fragile, which means that they intrinsic properties can often only be observed in extremely pure crystals. Under this respect, a great role is held by the Ruddlesden-Popper (*R-P*) series of $Sr_{n+1}Ru_nO_{3n+1}$ strontium ruthenates, fascinating example of nature's engineer layered systems whose properties can be dramatically tuned by impurities and disorder. The typical structure of this class of compounds (see Figure 1) is made up of n consecutive perovskite layers ($SrRuO_3$) alternating with rocksalt layers (SrO) so that the formula can be written as $(SrO)(SrRuO_3)_n$. Since the discovery, nearly 40 years ago, of the distorted perovskite $SrRuO_3$ as a ferromagnetic metal with T_{curie}~160 K (Allen *et al.*, 1996), many studies of the R-P compounds have provided clear evidence

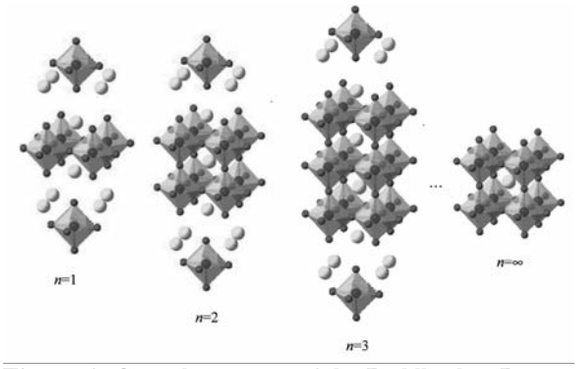

Figure 1. Crystal structure of the Ruddlesden–Popper series of $Sr_n+1Ru_nO_{3n}+1$ with n=1, 2, 3, and ∞.

that one of the most striking features of these oxides is that they display varying functionalities as the number of Ru-O layers per unit cell, n, increases (Cao *et al.*, 1999). Besides the unconventional spin triplet superconductor Sr_2RuO_4 (n=1) (Mackenzie and Maeno, 2003), the *R-P* series also includes the n=2 bilayered member, $Sr_3Ru_2O_7$ (Perry *et al.*, 2004), which is a metamagnetic normal metal with a quantum critical point, the nearly ferromagnetic $Sr_4Ru_3O_{10}$ (n=3) (Crawford *et al.*, 2002; Cao *et al.*, 2003b) and the itinerant ferromagnet $SrRuO_3$ (n=∞) (Mazin and Singh, 1997). In general, all the strontium ruthenates are metallic when they are grown in their stoichiometric forms and inclined to be magnetically ordered but small changes in either the crystal structure or the phase purity can switch their ground states all the way from correlated electron insulators to high-conductivity metals (Mackenzie and Y. Maeno, 2003; Nakatsuji and Y. Maeno, 2000; Grigera *et al.*, 2004). An outstanding example is the unconventional superconductivity observed in Sr_2RuO_4. This material, which is a close structural relative of high-temperature superconducting cuprates, is the first perovskite oxide superconductor with no copper. In contrast to most conventional superconductors which are largely immune to scattering from impurities or imperfections, the suppression of the superconducting transition temperature by non magnetic and magnetic impurities in this compound is one of the key signatures of its unconventional or non-s-wave superconductivity (Mackenzie *et al.*, 1998). The achievement of high quality samples is therefore a necessary prerequisite for the new superconducting state in Sr_2RuO_4 to be observed in the first place. Over the years, active investigations have been carried out to establish unambiguously the spin triplet superconductivity of Sr_2RuO_4. One of the major obstacle for understanding the physical properties of this ruthenate has been the lack of superconducting thin films. Tunnel experiments performed with superconductor-insulator-superconductor and superconductor-insulator-normal metal junctions based on Sr_2RuO_4 single crystals raised the crucial problem of controlling interfaces. The development of eutectic crystal growth of these systems has been proved to be an excellent route to merge together in a single composite crystal individual constituents with distinct physical properties thus offering the possibility to engineer new heterostructures with *ad hoc* functionalities. $Sr_3Ru_2O_7/Sr_2RuO_4$ eutectic crystals have been successfully grown by flux feeding floating zone technique (Fittipaldi *et al.*, 2004; Fittipaldi et al, 2008; Ciancio *et al.*, 2009). Such a composite structure, consisting of significant volume fractions of both Sr_2RuO_4 and the $Sr_3Ru_2O_7$, provides natural junctions and allows the study of tunnelling and proximity effect between the spin-triplet superconductor Sr_2RuO_4 and the nearly ferromagnetic metal $Sr_3Ru_2O_7$. The choice of $Sr_3Ru_2O_7$ as normal metal was driven by the high similarities in both the structural properties and growth conditions with the homologue Sr_2RuO_4: high purity single crystals of $Sr_3Ru_2O_7$ with a low residual resistivity comparable to that of Sr_2RuO_4 have been obtained. Such features represent a chance of a good crystalline matching at the interfaces with the possibility of good transport properties through the interfaces. Moreover it is worth to note that Sr_3RuO_7 is a really interesting compound in itself. $Sr_3Ru_2O_7$ was first found to be an anti-ferromagnetic metal (Cava *et al.*, 1997), then claimed as an enhanced paramagnetic metal with a changeover from paramagnetism to ferromagnetism under uniaxal pressure applied along its *c*-axis (Ikeda *et al.*, 2000). Lately $Sr_3Ru_2O_7$ has been reported as an itinerant metamagnet exhibiting quantum critical phenomena (Perry *et al.*, 2004). It is remarkable that no sign of superconductivity have been ever found even in the purest single crystals of $Sr_3Ru_2O_7$. During the course of the investigation of the functional properties of the $Sr_3Ru_2O_7/Sr_2RuO_4$ eutectics, an unexpected superconducting behaviour has been measured in the $Sr_3Ru_2O_7$ domain (Hooper *et al.*, 2006; Fittipaldi *et al.*, 2008; Kittaka *et al.*, 2008). Several

pictures have been proposed to explain this unusual behaviour such as a proximity effect (Hooper *et al.*, 2006) or, in analogy with the Ru-Sr_2RuO_4 eutectic system (Maeno *et al.*, 1998; Yaguchi *et al.*, 2003; Sigrist and Monien, 2001), the possible presence of an additional phase at the $Sr_3Ru_2O_7$ /Sr_2RuO_4 interfaces (Kittaka *et al.*, 2008). In this scenario, the investigation of the nanostructure of the $Sr_3Ru_2O_7$ domain of the Sr_2RuO_4- $Sr_3Ru_2O_7$ eutectic crystals is of crucial importance to extract the intrinsic properties of this ruthenate. This can be done by strictly comparing the nanostructure of the $Sr_3Ru_2O_7$ region of the eutectic with that of $Sr_3Ru_2O_7$ when it is grown as single phase crystal. Moreover, to verify weather the unexpected superconducting behaviour measured in the $Sr_3Ru_2O_7$ domain might be induced by the presence of an additional phase forming at the $Sr_3Ru_2O_7$ /Sr_2RuO_4 interfaces, it is crucial to determine atomic structure of the $Sr_3Ru_2O_7$ /Sr_2RuO_4 interfaces.

In this work, we provide a full characterisation of the nanostructures of the $Sr_3Ru_2O_7$/Sr_2RuO_4 eutectic crystals by transmission electron microscopy (TEM) and high angle annular dark field (HAADF) scanning TEM (STEM). A special emphasis is paid on the $Sr_3Ru_2O_7$ domain which is compared to $Sr_3Ru_2O_7$ grown as single phase material. A detailed characterisation of the atomic structure of the $Sr_3Ru_2O_7$/Sr_2RuO_4 interfaces is also provided.

Materials and Methods

The $Sr_3Ru_2O_7$/Sr_2RuO_4 eutectic crystals and the $Sr_3Ru_2O_7$ single phase crystals have been grown by flux feeding floating-zone technique with Ru self-flux, using a commercial image furnace equipped with double-elliptical mirrors and two 2.0 kW halogen lamps (NEC Machinery, model SC-K15HD-HP). An off-stoichiometric ratio k_{single}=1.6 and $k_{eutectic}$=1.45, respectively (where k=2N(Ru)/N(Sr), N(Ru) and N(Sr) being the mol fraction for Sr and Ru) was used to compensate the Ru evaporation during the crystal growth (R. Fittipaldi *et al.*, 2004). During the eutectic solidification, the $Sr_3Ru_2O_7$ and Sr_2RuO_4 phases solidify along the *b* direction in an ordered pattern consisting of alternating lamellae of thickness ranging from 60 to 200 μm piled up along the *c* direction. X-ray analysis showed only the presence of the Sr_2RuO_4 and $Sr_3Ru_2O_7$ phases which are fully aligned in the crystallographic directions (R. Fittipaldi *et al.*, 2004). Rietveld analysis of powdered eutectic crystals confirmed the previously determined ratio between the two phases. Although $Sr_3Ru_2O_7$ belongs to the orthorhombic space group Bbcb (Huang *et al.*, 1998; Shaked *et al.*, 2000), both Sr_2RuO_4 and $Sr_3Ru_2O_7$ can be considered as having a tetragonal crystal structure a=0.3862 nm and c=1.2722 nm, and a=0.38872 nm and c=2.0732 nm, respectively (Huang *et al.*, 1998; Chmaissem *et al.*,1998).

The TEM studies were performed using a Philips CM 200 field emission gun TEM with an attached Link ISIS EDS system and a Gatan Imaging Filter. HAADF analysis was carried out using a Titan 80-300 TEM/STEM with a probe spherical aberration corrector. Both instruments were operated at 200 kV. The HAADF images were recorded using a convergence semiangle of 24 mrad and a collection semiangle of 90 mrad giving Z contrast.

TEM specimens were extracted using a FEI Strata 235 DualBeam combined SEM and focused ion beam (FIB) instrument. 100-nm-thick TEM foils were thus obtained by a FIB-SEM liftout procedure and further thinned down to electron transparency by a Gatan Precision Ion Polishing System equipped with two Ar sources.

Results and Discussion

The image of Figure 2 taken by Polarized Light Optical Microscope (PLOM) gives an overview of the $Sr_3Ru_2O_7$/Sr_2RuO_4 lamellar pattern in the *a*-*c* plane. As further confirmed by Energy Dispersive Spectroscopy analysis carried out by Scanning Electron Microscopy (Ciancio *et al.*, 2009a; Ciancio *et al.*, 2009b), the dark contrast stripes are Sr_2RuO_4 lamellae embedded in the brighter contrast $Sr_3Ru_2O_7$ matrix. To explore the nanostructure of the $Sr_3Ru_2O_7$ domain of the eutectic thin membranes suitable for TEM analysis were extracted from the bulk crystals by the above mentioned lift-out technique. In Figure 3a a HRTEM micrograph taken in the [010] zone axis of the $Sr_3Ru_2O_7$ domain of the eutectic is displayed. As shown in the image, the crystal fragment has a well ordered nanostructure with no sizeable changes in the atom arrangement. The typical atomic layer stacking of the $Sr_3Ru_2O_7$

phase constantly repeat all over the sample with a 2-nm-long periodicity corresponding to the *c*-axis value of the $Sr_3Ru_2O_7$ phase. Occasionally in the $Sr_3Ru_2O_7$ matrix layered defects identified by HAADF-STEM analysis as Sr_2RuO_4 layers (see Figure 3b) are observed which are distributed in a extremely small volume fraction and over distances of more than 50 nm from each other. This is confirmed by selected area electron diffraction (SAED) carried out over several regions of the sample. The SAED pattern in Figure 3a reveals only the characteristic spots of the $Sr_3Ru_2O_7$ phase thus confirming that the presence of Sr_2RuO_4 is very diluted to give discernable spots in the electron diffraction.

In contrast to $Sr_3Ru_2O_7$ grown via eutectic solidification, the nanostructure of the $Sr_3Ru_2O_7$ single phase crystal has a disorder typical of intergrowths. The HRTEM micrograph of Figure 4a taken with the electron beam parallel to the [010] direction, enlightens the presence of thin slabs (indicated by arrows) with different atomic stacking intercalating within the $Sr_3Ru_2O_7$ matrix. A diffuse dark contrast is generally associated with these areas as a result of the strain originating at the slab edges because of the different atomic stacking of the embedded region with the respect to the surrounding matrix. As better emphasised by Figure 4b, in which a zoom-in of the defective region is displayed, such phases are planar faults of $SrRuO_3$ embedded in the $Sr_3Ru_2O_7$ matrix. In addition, randomly distributed one unit-cell and half unit-cell-thick layers of $Sr_4Ru_3O_{10}$ are observed. The presence of such intergrowths is clearly visible in the SAED pattern in the inset of Figure 4a which reveals the presence of additional spots beyond the characteristic reflections of the double-layered $Sr_3Ru_2O_7$ structure, indexed as those of the orthorhombic $Sr_4Ru_3O_{10}$ in the [010] zone axis. The stronger intensity of the $Sr_3Ru_2O_7$

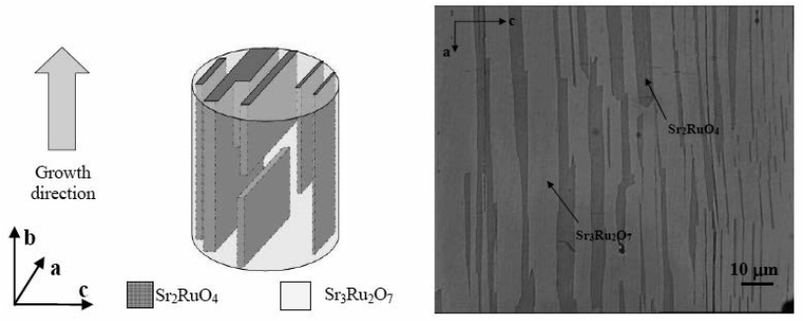

Figure 2. On the left a schematic drawing of the $Sr_2RuO_4/Sr_3Ru_2O_7$ eutectic crystal in which the three-dimensional lamellar structure is represented. On the right, an image taken by polarized light optical microscope of the $Sr_2RuO_4/Sr_3Ru_2O_7$ lamellar pattern in the *a-c* plane is shown (Ciancio *et al.*, 2009b, Ciancio *et al.*, 2010).

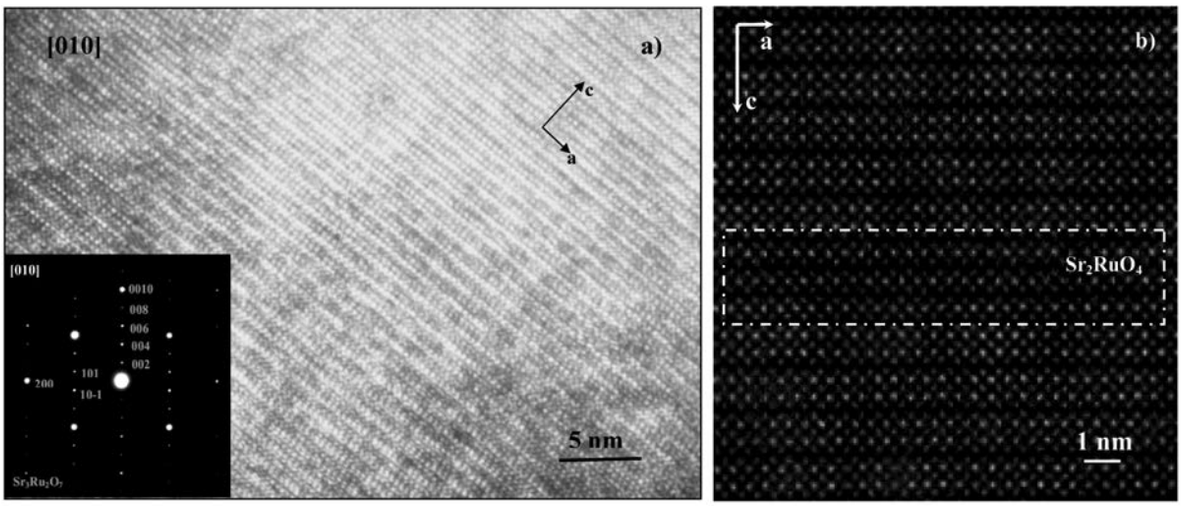

Figure 3. (a) HRTEM micrograph in the [010] zone axis showing the well-ordered atom arrangement of the $Sr_3Ru_2O_7$ region of the eutectic. (b) HAADF-STEM image showing the presence of Sr_2RuO_4 stacking faults (enlighten by the dash-edged box) in the $Sr_3Ru_2O_7$ matrix (Ciancio *et al.*, 2009a).

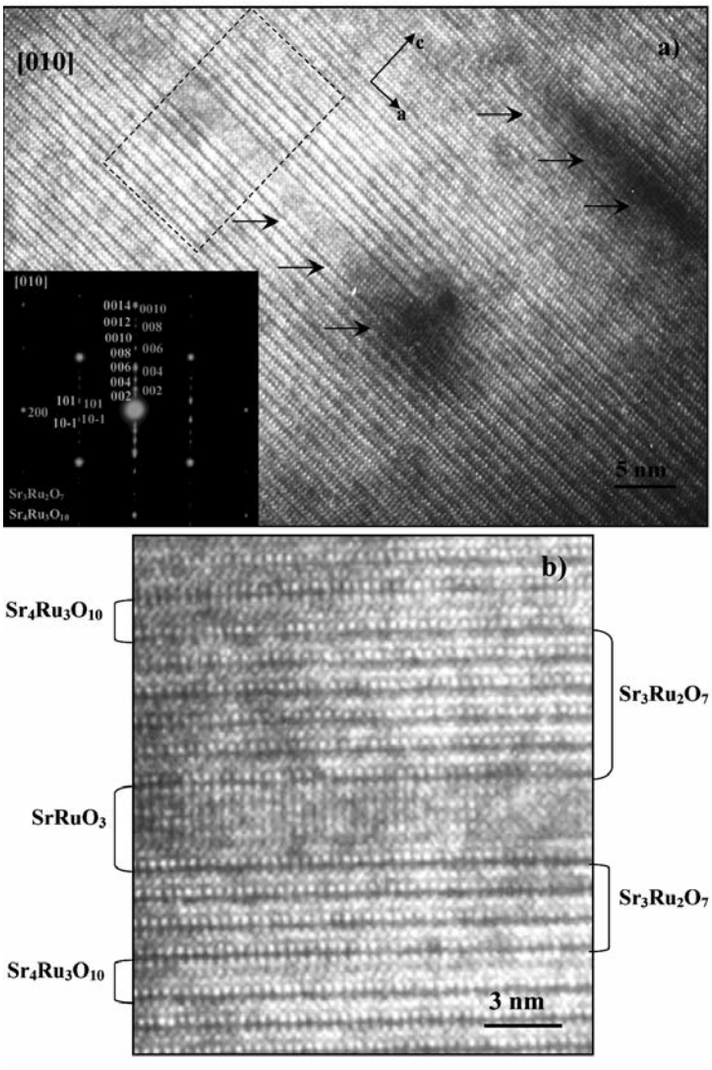

Figure 4. HRTEM micrographs of a $Sr_3Ru_2O_7$ single phase crystal taken in the [010] zone axis. In a) intergrowths of $SrRuO_3$ slabs intercalating within the $Sr_3Ru_2O_7$ matrix and associated with a diffuse dark contrast are indicated by arrows; in b) the defective region enlighten in a) by the dash-edged box is shown at higher magnification. A SrRuO3 slab and isolated half unit-cell of $Sr_4Ru_3O_{10}$ are displayed (Ciancio *et al.*, 2009a).

spots indicates a predominant contribution of $Sr_3Ru_2O_7$ ordered volume in the sample. In addition, diffuse streaks running through the fundamental spots are also seen, indicating a two-dimensional lattice defect on the *a*-*b* plane due to the presence of the intergrowths. The above remarks underscore the higher purity of the $Sr_3Ru_2O_7$ grown via eutectic solidification in which no atomically layered spurious phases are seen except for intergrowths of Sr_2RuO_4 occurring in very localized regions with poorly ordered volume to yield detectable spots in either XRD or electron diffraction. The statistics carried out on several representative regions showed that the total volume fraction of the Sr_2RuO_4 intergrowths is less than 5% of the imaged volume. The higher purity of the $Sr_3Ru_2O_7$ domain of the eutectic compared to $Sr_3Ru_2O_7$ single crystals, ascertained at atomic scale by TEM, is representative of the bulk samples, as confirmed by the magnetic measurements (Ciancio *et al.*, 2009) which reveal the presence of the magnetic transitions of the $SrRuO_3$ and $Sr_4Ru_3O_{10}$ phase.

The determination of the $Sr_3Ru_2O_7/Sr_2RuO_4$ interfacial nanostructure is another crucial point to be addressed to shed light on the unusual superconductivity measured in the eutectic. In particular, one of the crucial question to be answered is weather an additional phase might occur at the $Sr_3Ru_2O_7/Sr_2RuO_4$ interfaces thus justifying the insurgence of an additional superconductivity. As clearly shown in the PLOM image of Figure 2, the eutectic material provides two distinct typologies of interfaces namely along the *a* and *c* directions of the crystal. To explore the interfacial nanostructure in the two different orientations, cross sec-

tional samples were extracted by lift-out at the two interfacial regions and then analysed by TEM and HAADF-STEM (Ciancio *et al.*, 2009b). Our analysis revealed that the two interfacial regions have different nanostructures depending on their crystallographic orientation. As shown in the low magnification HRTEM micrographs of Figure 5, the interface parallel to the *a*-direction (Figure 5a) linearly proceeds over large distances and no elemental segregation can be seen across or in the vicinity of this region. However, the interface parallel to the *c*-axis (Figure 5b) is wavy over all the interfacial area with an amplitude of 50 nm. Defects and precipitates are distributed on either side of the interface over a 500 nm width region. The elemental segregation is higher on the Sr_2RuO_4 side appearing as a quite ordered distribution of nearly rectangular-shaped particles of dark contrast of a size ranging from 20 to 50 nm. EDS and HAADF analysis of the individual particles revealed that precipitates are Ru metal with hexagonal crystal structure. To completely rule out the possible presence of other phases at both $Sr_3Ru_2O_7$-Sr_2RuO_4 interfaces and to determine how the lattice interfacial match is built up, a more extensive characterisation was performed by STEM-HAADF. As shown in the HAADF image of Figure 6a taken in the [010] zone axis, the typical stacking of Sr_2RuO_4 (upper part) and $Sr_3Ru_2O_7$ (lower part) in the [010] direction can be discerned. The interface region is pointed by white arrows in the image. The brighter Ru columns are located in the center of the Sr–O columns with lower intensity. The matching at the interface between the two phases occurs with the sharing of the Sr–O rock salt, as shown in Figure 6b in which the white dash-edged region is shown aside the image at higher magnification with the corresponding labelling. The STEM-HAADF investigation was successful only in the case of the interfaces parallel to the *a*-axis. In the other case, the study was thwarted by the pronounced wiggling of the interface and by a consistent mismatch between the two phases. This can be seen by comparing the diffraction pattern taken in a defect-free area of the $Sr_3Ru_2O_7$ region in the [010] zone axis with that taken in a defect-free area of the Sr_2RuO_4 region keeping the tilt conditions of the $Sr_3Ru_2O_7$ region The SAED pattern corresponding to the Sr_2RuO_4 phase result to be out from his own [010] zone axis. Considering that the TEM sample holder allows the tilt of the specimen around two independent directions which are parallel to the in-plane crystallographic axis and a tilt of the specimen of 5° around the *a*-axis direction leads to the zone axis condition for the Sr_2RuO_4, the b axes of the two cells are tilted with respect to each other of about 5° around the *a*-axis direction. Such a misalignment only occurs in the *a*-*c* plane, where the two Sr_2RuO_4 and $Sr_3Ru_2O_7$ phase have to match along the *c*-axes which are different for the two cases. However, the lattice match along the *a*-axis is in an energetically favoured configuration because of the close values of the *a*-axis parameters of the two phases. As a consequence of such energy difference corresponding to the two interfacial orientations, it is understandable that elemental segregation only occurs at the interface parallel to the *c*-axis, where local change in chemical composition most likely can take place. These results are in a very good agreement with EBSD-SEM analysis performed on the bulk crystals (Ciancio *et al.*, 2010). In both cases no other phases are seen at the $Sr_3Ru_2O_7$/Sr_2RuO_4 interfaces thus ruling out the possibility of a superconductivity originated by the presence of additional phases at the $Sr_3Ru_2O_7$/Sr_2RuO_4 interfaces.

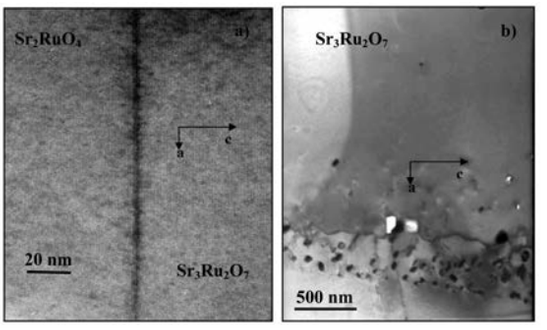

Figure 5. Overview of the two interfacial regions. In a) a TEM image taken in the [010] zone axis of the Sr_2RuO_4 /$Sr_3Ru_2O_7$ interfacial region with the interface along the *a* direction is shown. In b) a TEM micrograph in the [010] zone axis of the Sr_2RuO_4/$Sr_3Ru_2O_7$ interfacial region in which the wavy interface parallel to the *c* direction and the Ru precipitates (dark contrast particles) are seen (Ciancio *et al.*, 2009b).

Conclusions

Eutectic solidification has been proved to be a fruitful way to grow high quality crystals. In particular, we show that $Sr_3Ru_2O_7$ grown via eutectic solidification has a significantly lower amount of

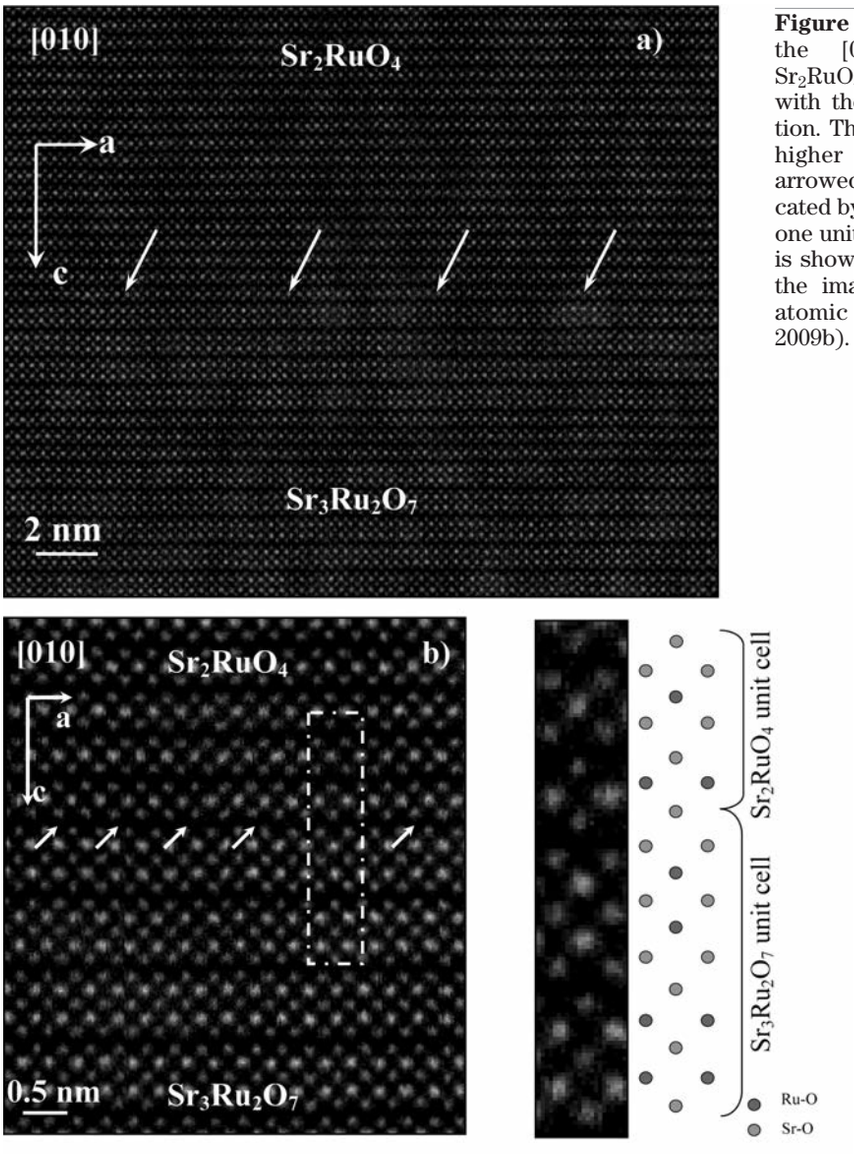

Figure 6. a) HAADF image taken in the [010] zone axis of the $Sr_2RuO_4/Sr_3Ru_2O_7$ interfacial region with the interface along the a direction. The interface region is shown at higher magnification in b) and arrowed. The area of the image indicated by the white rectangle, including one unit cell of Sr_2RuO_4 and $Sr_3Ru_2O_7$, is shown with higher resolution aside the image with a schematic of the atomic positions (Ciancio *et al.*, 2009b).

layered spurious phase compared to $Sr_3Ru_2O_7$ single phase crystals, where intergrowths of $Sr_4Ru_3O_{10}$ and $SrRuO_3$ are found. The diluted presence of Sr_2RuO_4 stacking faults in the $Sr_3Ru_2O_7$ region of the eutectic excludes a simple percolation via proximity effect to justify the observed supercurrent and points on the possibility of the achievement of longer mean free paths in $Sr_3Ru_2O_7$ grown via eutectic solidification which would enable a long range communication via Kondo effect between the finely dispersed Sr_2RuO_4 layers. The analysis of the interfacial nanostructure in the three crystallographic orientations addressed crucial aspects on both the crystal growth and the potential application of this eutectic for the fabrication of spin-triplet tunnel junctions. Our studies revealed that the interfaces have different nanostructure depending on their orientation with respect to the growth direction of the crystal. The interfaces parallel to the both *a* direction are straight and defect-free due to the 'easy-axis' matching (the *a* axis parameters, are the same for Sr_2RuO_4 and $Sr_3Ru_2O_7$). On the contrary, along the 'hard-axis' matching (*c*-axis, which differs of about 0.8 nm in the two oxides), the interfaces are wiggly and decorated with Ru particles. Our investigations revealed that these last interfaces are the best candidates for tunnel experiments to study the order parameter symmetry of Sr_2RuO_4. The occurring of such elemental segregation in a specific crystallographic orientation opens

the study of possible effects coming from the thermodynamic stability of this compound, such as the favourite energy surfaces, the phase formation dynamics, and the role of the active Ru evaporation during the growth. More in general, because of the high similarities between strontium ruthenates and other polymorphic oxides, these findings can be considered as representative of a wide class of materials and therefore applicable to the eutectic growth of other anisotropic oxide systems.

Acknowledgements

R. Ciancio gratefully acknowledges the Swedish Institute, the Blanceflor Boncompagni-Lodovisi Foundation, the "Angelo della Riccia" Foundation, and the ESF activity Thin Films for Novel Oxide Devices (THIOX) and the for partially supporting her research activity at Chalmers University of Technology.

References

Cao G, Alexander CS, McCall S, et al. From antiferromagnetic insulator to ferromagnetic metal: a brief review of the layered ruthenates. Mater Sci Eng B 1999;63:76-82.

Cao G, Balicas L, Song WH, et al. Competing ground states in triple-layered Sr4Ru3O10: Verging on itinerant ferromagnetism with critical fluctuations. Phys Rev B 2003;68:174409.

Cao G, McCall S, Crow JE. Observation of itinerant ferromagnetism in layered Sr3Ru2O7 single crystals. Phys Rev B 1997;55:R672-R675.

Cava RJ, Zandbergen RW, Krajewski JJ, et al. Sr2RuO4 · 0.25 CO2 and the Synthesis and Elementary Properties of Sr3Ru2O7. J. Solid State Chem. 1995;116:141-5.

Chmaissem O, Jorgensen JD, Shaked H, et al. Thermal expansion and compressibility of Sr2RuO4. Phys Rev B 1998;57:5067-70.

Ciancio R, Börjesson J, Pettersson H, et al. Toward intrinsic funtionalities of bilayered ruthenate Sr3Ru2O7. Phys Rev B 2009;80:054110.

Ciancio R, Pettersson H, Börjesson J, et al. Atomic structure of functional interfaces in Sr3Ru2O7/Sr2RuO4 eutectic crystals. Appl Phys Lett 2009;95:142507.

Ciancio R, Pettersson H, Fittipaldi R., et al. Electron Backscattering Diffraction and X-ray Diffraction studies of interface relationships in Sr3Ru2O7/Sr2RuO4 eutectic crystals. Micron 2010 in press.

Crawford M, Harlow RL, Marshall M, et al. Structure and magnetism of single crystal Sr4Ru3O10:A ferromagnetic triple-layer ruthenate. Phys. Rev B 2002; 65:214412.

Fittipaldi R, Vecchione A, Ciancio R, et al. Superconductivity in Sr2RuO4-Sr3Ru2O7 eutectic crystals. Europhys Lett 2008;83:27007.

Fittipaldi R, Vecchione A, Fusanobori S, et al. Crystal growth of the new Sr2RuO4–Sr3Ru2O7 eutectic system by a floating-zone method. J Cryst Growth 2004;271:152-9.

Grigera SA, Gegenwart P, Borzi RA, et al. Disorder-Sensitive Phase Formation Linked to Metamagnetic Quantum Criticality. Science 2004;306:1154-7.

Hooper J, Zhou M, Mao ZQ, et al. Critical current of the Sr2RuO4-Sr3Ru2O7 eutectic system. Phys Rev B 2006;73:132510.

Huang Q, Lynn JW, Erwin RW, et al. Oxygen displacements and search for magnetic order in Sr3Ru2O7. Phys Rev B 1998;58:8515-21.

Ikeda SI, Maeno Y, Nakatsuji S, et al. Ground state in Sr3Ru2O7: Fermi liquid close to a ferromagnetic instability. Phys Rev B 2000;62:R6089-R6092.

Kittaka S, Fusanobori S, Yonezawa S, et al. Multiple superconducting transitions in the Sr3Ru2O7 region of Sr3Ru2O7-Sr2RuO4 eutectic crystals. Phys Rev B 2008;77:214511.

Mackenzie AP, Maeno Y. The superconductivity of Sr2RuO4 and the physics of spin-triplet pairing. Rev Mod Phys 2003;75:657-712.

Maeno Y, Ando T, Mori Y, et al. Enhancement of Superconductivity of Sr2RuO4 to 3 K by Embedded Metallic Microdomains. Phys Rev Lett 1998;81:3765-68.

Mazin II, Singh DJ. Electronic structure and magnetism in Ru-based perovskites. Phys Rev B 1997;56:2556-71.

Nakatsuji S, Maeno Y. Quasi-Two-Dimensional Mott Transition System Ca2-xSrxRuO4. Phys Rev Lett 2000;84:2666-9.

Perry RS, Kitagawa K, Grigera SA, et al. Multiple First-Order Metamagnetic Transitions and Quantum Oscillations in Ultrapure Sr3Ru2O7. Phys Rev Lett 2004;92:166602.

Shaked H, Jorgensen JD, Chmaissem O, et al. Neutron Diffraction Study of the Structural Distortions in Sr3Ru2O7. J. Solid State Chem 2000;154:361-7.

Sigrist M, Monien HJ. Phenomenological Theory of the 3 Kelvin Phase in Sr2RuO4. J Phys Soc Jpn 2001; 70:2409-18.

Yaguchi H, Wada M, Akima T, et al. Interface superconductivity in the eutectic Sr2RuO4-Ru: 3-K phase of Sr2RuO4. Phys Rev B 2003;67:214519.